JCB Article

The carboxyl-terminal isoforms of smooth muscle myosin heavy chain determine thick filament assembly properties

Arthur S. Rovner, Patricia M. Fagnant, Susan Lowey, and Kathleen M. Trybus

Department of Molecular Physiology and Biophysics, University of Vermont, Burlington, VT 05405

The alternatively spliced SM1 and SM2 smooth muscle myosin heavy chains differ at their respective carboxyl termini by 43 versus 9 unique amino acids. To determine whether these tailpieces affect filament assembly, SM1 and SM2 myosins, the rod region of these myosin isoforms, and a rod with no tailpiece (tailless), were expressed in Sf 9 cells. Paracrystals formed from SM1 and SM2 rod fragments showed different modes of molecular packing, indicating that the tailpieces can influence filament structure. The SM2 rod was less able to assemble into stable filaments than either SM1 or the tailless rods. Expressed full-length SM1 and SM2 myosins showed solubility differences comparable to the rods, establishing the validity of the latter as a model for filament assembly. Formation of homodimers of SM1 and SM2 rods was favored over the heterodimer in cells coinfected with both viruses, compared with mixtures of the two heavy chains renatured in vitro. These results demonstrate for the first time that the smooth muscle myosin tailpieces differentially affect filament assembly, and suggest that homogeneous thick filaments containing SM1 or SM2 myosin could serve distinct functions within smooth muscle cells.

Introduction

The vertebrate smooth muscle myosin heavy chain is encoded by a single gene, but alternative splicing at two sites can create four different variants of this ~200-kD polypeptide. The first identified splice site occurs near the tip of the coiled-coil myosin tail, and gives rise to variants containing either 43 (SM1) or 9 (SM2) unique carboxyl-terminal residues that are predicted to be nonhelical (Babij and Periasamy, 1989; Nagai et al., 1989). The protein variants corresponding to these messages are ubiquitous in adult smooth muscles (Rovner et al., 1986b). The longer SM1 isoform appears developmentally earlier than SM2 in most mammals (Mohammad and Sparrow, 1988; Eddinger and Wolf, 1993), and its expression is maintained during the proliferative phase of cell culture, whereas SM2 expression ceases (Rovner et al., 1986a). These distinct patterns of expression suggest unique roles for the two isoforms in smooth muscle cell function, but a clear difference in properties between them has yet to be established in vitro.

Nonhelical tailpieces are present in a variety of nonmuscle myosin IIs, and in many cases they are involved in the regulation of filament assembly or enzymatic activity. In mammals, assembly of the B isoform of rabbit brain myosin is strongly inhibited by protein kinase C phosphorylation of a residue in the nonhelical tailpiece (Murakami et al., 1998). In the myosin of the amoeba *Dictyostelium*, the carboxyl-terminal region of the tail is required for proper regulation of myosin filament assembly and enzymatic activity (O'Halloran et al., 1990), whereas in *Acanthamoeba*, phosphorylation of the tailpiece regulates enzymatic activity, despite its distance from the active site (Atkinson and Korn, 1987; Sathyamoorthy et al., 1990).

Analysis of bacterially expressed truncated light meromyosin (LMM)* fragments from chicken intestinal epithelium brush border myosin, which has a nonhelical tailpiece similar to SM1, showed that the tailpiece enhances filament assembly (Hodge et al., 1992). Conversely, proteolytic removal of the SM1 tailpiece from purified chicken gizzard myosin was reported to enhance filament formation (Ikebe et al., 1991). Both of these studies suggested that the tailpiece influences

Address correspondence to Arthur S. Rovner, Department of Molecular Physiology and Biophysics, University of Vermont, Burlington, VT 05405. Tel.: (802) 656-8004. Fax: (802) 656-0747. E-mail: rovner@physiology.med.uvm.edu

Key words: cytoskeleton; myosin heavy chains; smooth muscle; sarcomeres; uterine contraction

*Abbreviations used in this paper: Gu-HCL, guanidine hydrochloride; HIS hexa-histidine; HMM, heavy meromyosin; IMAC, immobilized metal affinity chromatography; LMM, light meromyosin; TL, tailless.

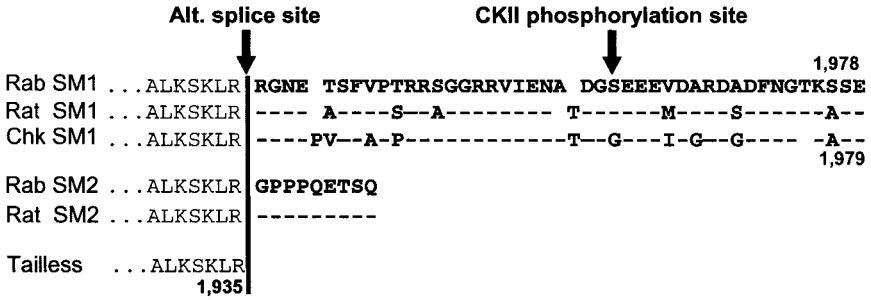

Figure 1. **Carboxyl-terminal sequences of SM1 and SM2 isoforms from different vertebrates.** The mammalian SM1 heavy chains are 1,978 residues in length, whereas the chicken isoform is 1,979 due to an extra residue in its tailpiece. The TL mutant was truncated after the Arg residue immediately preceding the alternative splice site at residue 1,935. The labeled serine is phosphorylated by casein kinase II (CKII) in mammalian cells (Kawamoto and Adelstein, 1988).

assembly, but a consistent trend was not revealed, nor did they directly compare the filament assembly properties of myosin containing the two naturally occurring isoforms found in smooth muscle cells.

The backbone of each myosin molecule is formed by the α-helical coiled-coil association of two heavy chains, so the question arises as to whether the SM1 and SM2 variants can form heterodimers. Large quantities of heterodimer in the cell would weaken the argument that the carboxyl-terminal isoforms differentially regulate assembly, as filaments containing the heterodimer would necessarily contain both SM1 and SM2 heavy chains. Earlier attempts to address this question have given conflicting answers. Immunological techniques showed that bovine aorta and chicken gizzard myosins exclusively form homodimers (Kelley et al., 1992). Conversely, a second group concluded that homo- and heterodimers were randomly formed in a number of tissues from different species, using gel analysis of cross-linked molecules (Tsao and Eddinger, 1993). Resolution of this conflict will be necessary before embarking on potential localization of tailpiece isoforms within the cell.

Here, we used baculoviral expression to prepare homogeneous populations containing either the SM1 or SM2 tailpiece. These constructs were used to compare the effects of the two different tailpieces on the intermolecular interactions which occur in ordered paracrystals, as well as on thick filament solubility and length. Differential tagging was also used to determine whether homodimers or heterodimers are the predominant species of coiled coil formed in vivo. We conclude that the tailpieces confer distinct filament assembly properties on myosin, and that the preferred formation of homodimers in vivo will allow for the functional distinction of these isoforms. Because the rate of cell shortening and force production of smooth muscles ultimately depend on how the filaments are arranged in the cell, the observation that tailpieces affect filament assembly implies that they could modulate smooth muscle cell physiology.

Results

Using the baculovirus system, we produced full-length smooth muscle myosin molecules and rod fragments containing the SM1 or SM2 tailpiece, as well as a rod fragment, named tailless (TL), whose sequence was terminated at the alternative splice site (Fig. 1). The high yields of the expressed rod fragments, along with their ability to form paracrystals, made them the molecules of choice for most of our filament assembly assays. Although the lower yields of the full-length myosins precluded a complete analysis of their properties, we obtained a limited data set which duplicated the trends observed with the rod isoforms, thus validating the rod as a model for tailpiece effects on myosin assembly.

Expressed rod heavy chain isoforms retain their carboxyl termini

The tailpieces of smooth muscle myosin heavy chain isoforms are susceptible to proteolytic degradation, so it was important to verify that the carboxyl termini of expressed constructs were retained during expression and purification. Electrophoresis on low percentage acrylamide gels demonstrated wide separation of rod SM1 and SM2, whereas TL had mobility slightly greater than that of SM2, as demonstrated in the coelectrophoresis lane 4 (Fig. 2, top). Western blotting of an identically loaded gel with an SM2-specific monoclonal antibody showed recognition of rod SM2, but not SM1 or TL (Fig. 2, bottom). These results confirmed that each of the expressed molecules retained its unique carboxyl-terminus throughout purification, and that any functional differences we observed were due to these sequences.

SM1 and SM2 paracrystals show different molecular packing

Electron microscopic examination of the paracrystalline structures formed by rod SM1 and SM2 revealed striking differences, suggesting different modes of molecular packing. The segments formed by rod SM1 were generally very long, narrow needles, whereas those formed by SM2 appeared flatter, wider, and more branched. SM1 paracrystals showed a constant repeat distance of ~64 nm (Fig. 3 A) comprised of alternating light-staining bands of 43 nm, and dark-staining bands 21.5 nm in width. SM2 exhibited very narrow (<1

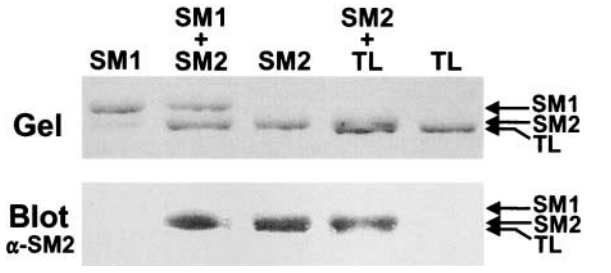

Figure 2. **Electrophoretic separation of the expressed rod carboxyl-terminal isoforms.** (Top) Coomassie blue–stained 5% acrylamide gel loaded as labeled. (Bottom) Identically loaded lanes after transfer to nitrocellulose, and reaction with a monoclonal antibody specific for the SM2 tailpiece.

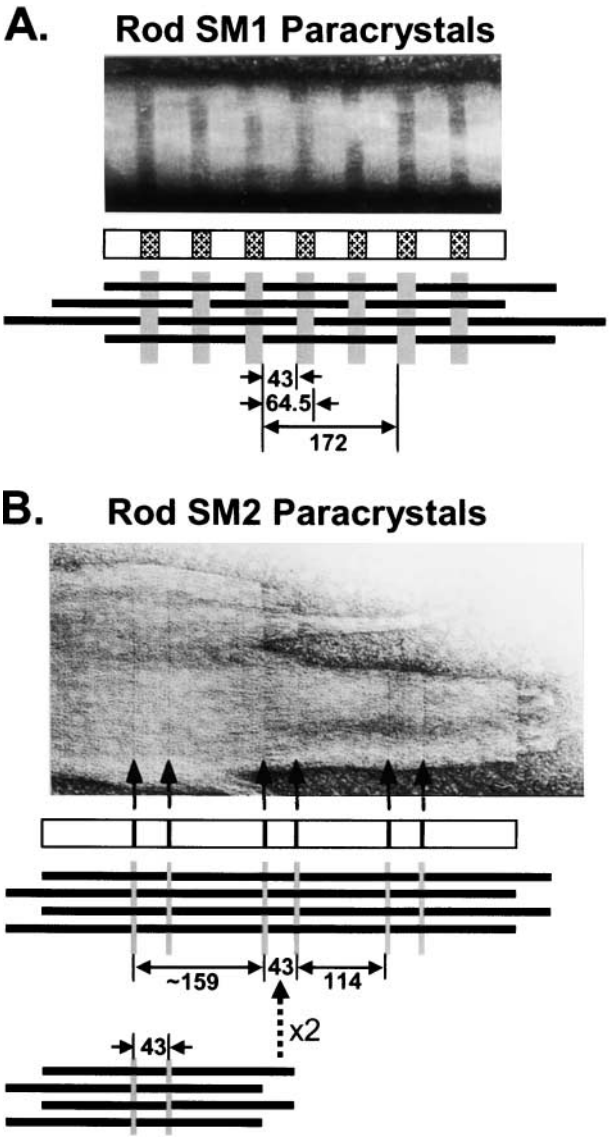

Figure 3. **Electron micrographs and derived models for paracrystals of rod SM1 and SM2.** Negatively stained rod paracrystals were viewed at magnifications of 50–60,000×, and the lengths of dark- and light-staining bands were measured as described in Materials and methods. In the packing models below the paracrystals, thick black lines represent the rod fragments, whereas shaded gray rectangles represent gaps where stain has deposited. (A) The approximate lengths of the light-staining region, an entire repeat, and one molecule of rod SM1 are illustrated with arrows. (B) The compound segment of rod SM2 (upper portion of model) is formed by the end-to-end annealing of two (or more) segments with 43 nm staggers (vertical arrow between lower portion and upper portion of model). Lengths of a single molecule, the central overlap zone, and the longer staggered region of the rod, respectively, are indicated on the upper portion of the model.

nm) bands of dark stain, which defined light-staining, alternating zones of 43 and ~114 nm in width (Fig. 3 B). Paracrystals of TL were qualitatively similar to those formed by SM2, with very narrow dark bands defining light-staining regions of two different lengths (unpublished data).

The wider, dark-staining band in SM1 paracrystals suggested that the longer tailpiece acts as a spacer, creating a greater area for stain to penetrate between successive molecules. The similarity of the narrow dark bands seen for paracrystals formed from the shorter SM2 tailpiece or with TL suggests that the smaller tailpiece does not have much effect on the gaps between the molecules, although both differ significantly from the SM1 paracrystals. The SM2 and TL structures which we observed closely resemble end-to-end aggregates of the bipolar segments formed by proteolytically derived rod from chicken gizzard myosin (Kendrick-Jones et al., 1971), which is likely to be lacking a tailpiece.

Tailpieces affect thick filament lengths and stability

The different modes of packing observed in the paracrystals led us to examine how the tail isoforms might affect the properties of filaments formed under more physiological solvent conditions. The combined results of the filament length analyses indicate that either type of smooth muscle tailpiece inhibits thick filament elongation compared with the situation where a tailpiece is lacking. The length distributions of rod SM1 and SM2 filaments in buffer containing 4 mM $MgCl_2$ at pH 7.5 were similar, and gave average length values only 3% different from each other (Fig. 4, A and B; Table I). TL formed significantly longer filaments (~50% greater than SM1 and SM2, respectively), and showed a much wider distribution of lengths than the tailpiece isoforms (Fig. 4 C). Over 6% of the TL filaments were >2 μm in length.

The average lengths of filaments formed by each of the rods at pH 8.0 in the absence of $MgCl_2$ were 50–75% as long as those formed at pH 7.5 with 4 mM $MgCl_2$ (Table I). Under these stringent conditions, the amount of variation of lengths around the mean value was strikingly less than at the lower pH. TL again formed longer filaments under these conditions, but in this case it was only 6% longer than SM1 and 10% longer than SM2.

The salt-dependent solubility of the three rod fragments was assessed under the same conditions as those used for electron microscopy. At pH 7.5, in the presence of 4 mM $MgCl_2$, SM1 and SM2 rods had nearly the same solubilities, whereas TL was more filamentous at all salt concentrations (Fig. 5 A). When assembly was discouraged by raising the pH to 8.0 and omitting $MgCl_2$, there was a small but highly reproducible increase in the ability of SM1 to form filaments compared with SM2 over the range of NaCl concentrations from 125 to 170 mM (Fig. 5 B). The tendency to form filaments followed the order TL>SM1>SM2.

The greater solubility of SM2 suggested that its critical concentration for filament assembly was higher than either SM1 or TL. To support this conclusion, we measured the amount of rod monomer in equilibrium with polymer for rod SM1, SM2, and TL at pH 8.0 and 150 mM NaCl, as a function of total rod concentration (Fig. 5 C). For rod SM2, the amount of soluble protein increased as more total rod protein was added to the assay until the curve leveled off at ~65 μg/ml monomer, indicating that this was the critical concentration threshold for filament assembly. Conversely, the curves for SM1 and TL plateaued at values of ~15 and 30 μg/ml. These results indicate that TL and SM1 form filaments at protein concentrations 2.5–4-fold less than SM2, and explain the greater tendency of SM1 and TL to assemble into filaments.

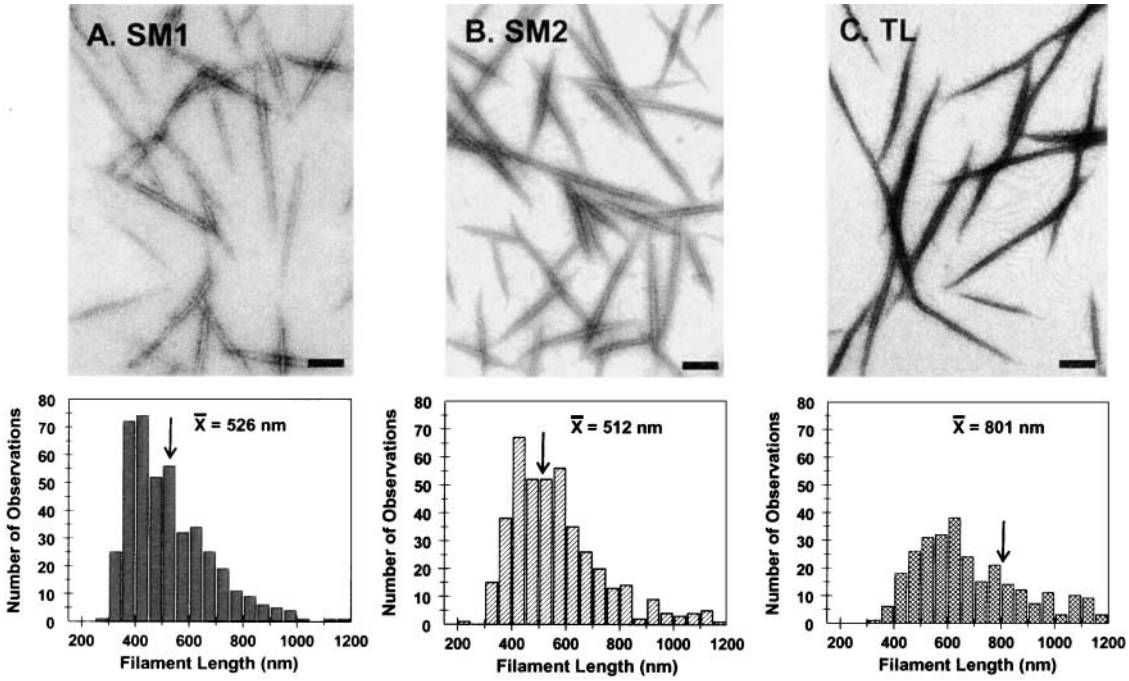

Figure 4. **Rod isoform thick filaments and length distribution analysis.** Thick filaments formed in 4 mM $MgCl_2$ at pH 7.5 were quantified digitally from electron microscopic negatives as described in Materials and methods. (Top) Photomicrographs of thick filaments. (Bottom) Histograms of filament lengths using bin sizes of 50. The average length of the population ($\bar{x}$) is indicated by the vertical arrow in each panel. (A) Rod SM1; (B) Rod SM2; (C) TL. Bars, 200 nm.

Rod is a good model for myosin assembly

It was important to demonstrate that the relative filament assembly behaviors of full-length myosin SM1 and SM2 were similar to rod SM1 and SM2, to ensure that the latter serve as valid models for the former. After expression and isolation, electrophoresis of the myosins on 3.5% acrylamide SDS gels showed that the mobility of the SM1 heavy chain was slightly less than that of the expressed SM2 (Fig. 6 A). The positions of the expressed isoforms on the gel were identical to the two heavy chain variants seen in a fresh extract of chicken gizzard tissue, indicating there had been no proteolytic clipping of their carboxyl termini. Thick filaments of full-length myosin formed by rapid dilution in a buffer with pH 7.2 and 4 mM $MgCl_2$ closely resembled those formed by the rod fragments under similar conditions, displaying a heterogeneous distribution of filament lengths (Fig. 6 B).

The expressed SM1 and SM2 myosins were indistinguishable in their ability to move actin in an unloaded in vitro motility assay (Fig. 7 A). The velocities were the same as those obtained for myosin isolated from tissue, indicating that the expressed molecules have retained good functionality throughout purification. Like the rod fragments, the solubility of SM1 and SM2 myosins at pH 7.5 in the presence of 4 mM $MgCl_2$ was nearly the same over a range of salt concentrations (Fig. 7 B). We also assessed the critical concentration of SM1 and SM2 myosin at 160 mM NaCl and pH 8.0, where the greatest differences between the rod isoforms were apparent. The critical concentration of assembly for myosin SM1 was 5 μg/ml, compared with a value of ~30 μg/ml for SM2, nearly duplicating the four- to five-fold greater stability of SM1 rod compared with SM2 rod. Therefore, the comparable trends in assembly we obtained strongly suggest that the expressed rod fragments accurately model the filament assembly behavior of the intact molecule.

Rod homodimer formation is favored in living cells

The potential impact of tailpiece isoforms on filament assembly will be much greater if single molecules preferentially contain the same tailpiece, as this would allow the formation

Table I. **Lengths of thick filaments formed by SM1, SM2, and TL rods**

	pH 7.5 + 4 mM $MgCl_2$			pH 8.0		
	$\bar{X}$ (nm)	SEM	N	$\bar{X}$ (nm)	SEM	N
SM1	526[a]	7.7	430	386[ab]	4.1	389
SM2	512[a]	12.4	428	372[a]	3.5	573
TL	801	22.1	322	409	5.8	316

Thick filaments were polymerized by rapid dilution or dialysis into a final salt concentration of 150 mM NaCl, and lengths were then analyzed as described in Materials and methods. Listed are the average length ($\bar{x}$), the standard error of the mean (SEM), and the number of filaments measured (N) for each of the expressed rods.

[a]Significantly different from TL.

[b]Significantly different from SM2.

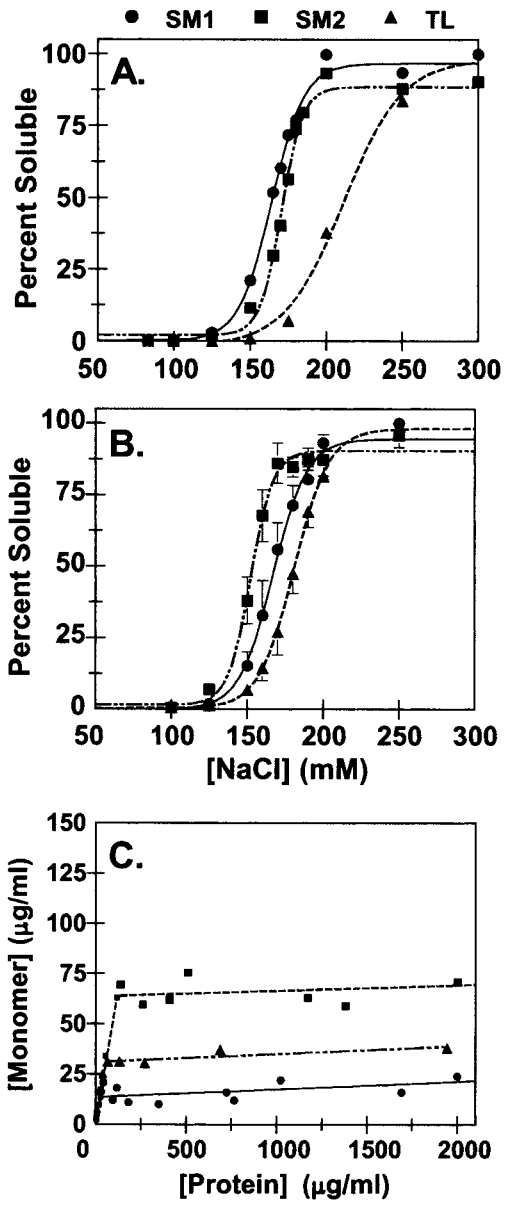

Figure 5. **Thick filament solubility for the three expressed rods.** (A) Solubilities of rod SM1, SM2, and TL at different concentrations of NaCl at pH 7.5 in the presence of 4 mM $MgCl_2$ were calculated as described in Materials and methods. The data presented is the average of two assays for SM1 and SM2, whereas TL is from a single assay. (B) Solubilities at different salt concentrations at pH 8.0 in the absence of $MgCl_2$. Values are averages of three to five different assays ± the standard deviation. (C) Critical concentrations for the three rods at pH 8.0 in the absence of $MgCl_2$. Total and monomer concentrations were derived by quantitative gel electrophoresis. Data in the plateau portion of the graph were fitted to the equation $y = mx + b$, where the intercept b gave the critical concentration value.

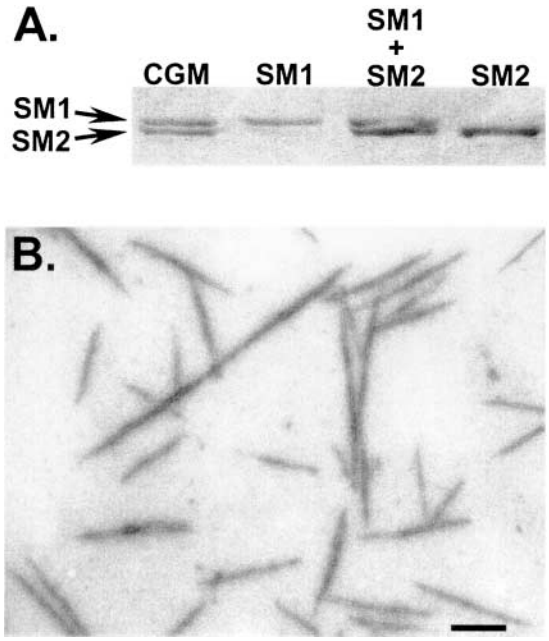

Figure 6. **Expressed full-length smooth muscle myosins.** (A) 3.5% acrylamide gel showing separation of SM1 and SM2 myosins. The lane labeled CGM is a fresh homogenate of chicken gizzard tissue, showing nearly equal amounts of myosin SM1 and SM2. (B) Electron micrograph of thick filaments of SM2 myosin in 150 mM NaCl, 1 mM EGTA, 10 mM Imidazole-HCl, pH 7.2, and 4 mM $MgCl_2$. Bar, 400 nm.

of distinct pools of homogeneous thick filaments with different functional properties. To determine whether this is the case in vivo, we compared the amount of rod SM1 or SM2 homo- and heterodimers produced in living cells with that formed upon renaturation of the two heavy chain isoforms from guanidine hydrochloride (Gu-HCl). Insect cells were coinfected with a combination of rod SM1 (hexa-histidine [HIS]-tagged) and SM2 (untagged) heavy chain viruses (see Materials and methods). This allowed the cells to synthesize untagged SM2/SM2 homodimers, singly tagged SM1/SM2 heterodimers, and doubly tagged SM1/SM1 homodimers. Fig. 8 illustrates a typical experiment in which the expressed native rod protein contained 38% SM1 and 62% SM2 rod, as determined by densitometry of the illustrated gel. This material was either directly loaded onto a metal ion chelation column or denatured in Gu-HCl, and then renatured before column purification (see Materials and methods). In both cases, identical quantities of protein were loaded on columns of identical size, and then washed with a buffer containing 10 mM imidazole to remove nonspecifically bound SM2. The imidazole gradient elution was then carried out by the same protocol, including flow rates and volumes of the fractions collected, so that the results could be directly compared between the native and renatured trials.

There was a clear difference in the two elution patterns (Fig. 8). Most of the protein obtained from the denaturation/renaturation experiment eluted much earlier in the gradient than the protein obtained from the in vivo expression. Because the doubly tagged SM1 homodimer elutes at higher imidazole concentrations than the singly tagged heterodimer, this observation shows a clear bias towards homodimer formation in vivo compared with in vitro. Moreover, the ratio of SM1/SM2 heavy chain is near equal in the majority of the fractions from the denaturation/renaturation experiment, whereas the later eluting fractions obtained from the in vivo experiment contain a preponderance of the SM1 heavy chain (Fig. 8). These results indicate that the formation of homodimeric coiled coils is favored in the living cell.

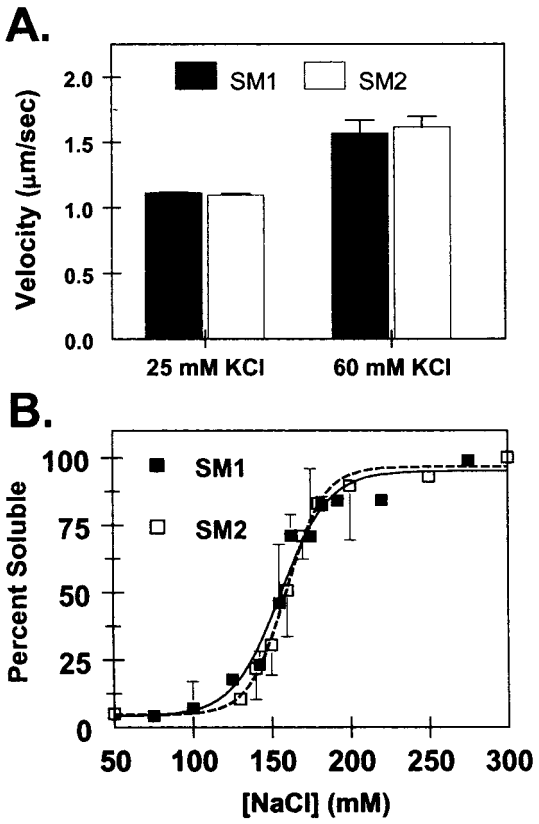

Figure 7. **Functional assessments of expressed myosin isoforms.** (A) In vitro actin filament motility supported by SM1 and SM2 myosins. Preparations were applied to the motility surface in monomeric form. Values are averages of two different preparations for 25 mM KCl and three different preparations for 60 mM KCl ± the standard deviation. (B) Comparative salt-dependent solubilities of SM1 and SM2 myosins at pH 7.5 in the presence of 4 mM $MgCl_2$. Values with error bars are averages of two to four different assays ± the standard deviation.

Homodimeric myosins could form heterogeneous thick filaments as long as the two isoforms can copolymerize. We tested this possibility by specifically labeling expressed SM1 and SM2 rods at their single cysteine residue with fluorescein and rhodamine, respectively, and then inducing them to form extremely long thick filaments by dialysis into a low-pH, low-salt buffer. Homogeneous preparations of rod SM1 or SM2 formed easily discernible filaments when viewed by epifluorescence with the appropriate filter set, but the same field of view had no fluorescence in the other filter (Fig. 9). When filaments were formed from a 50:50 mixture of the two rod types, they were in every case visible with both fluorescein and rhodamine filters, with comparable fluorescence intensities (Fig. 9). The same result was obtained when SM1 was labeled with rhodamine and SM2 was labeled with fluorescein. Thus, in vitro, molecules with the two tailpieces can copolymerize within a single filament.

Discussion

Smooth muscles can vary in shortening velocity by as much as 20-fold (Malmqvist and Arner, 1991; for review see Murphy et al., 1997), but the molecular basis for this large physiological difference has not been established. In striated muscles, myosin isoform variation can be directly related to differences in performance at the tissue level (Barany, 1967), so it is reasonable to suggest that the same may be true in smooth muscles. If so, then smooth myosin isoforms formed by alternative splicing: (a) at the carboxyl-terminus of the essential light chain; (b) in the surface loop at the entrance to the nucleotide pocket; or (c) at the extreme carboxyl terminus of the rod, should be able to generate such a wide range of performance. Earlier studies by ourselves and others showed that the essential light chain isoforms had no effect on the actin velocity supported by phosphorylated smooth muscle heavy meromyosin (HMM) in an in vitro motility assay, whereas the 7 amino acid insertion near the active site doubled this rate (Kelley et al., 1993; Rovner et al., 1997). This biochemical work may underestimate the effect of the insert in vivo, as a study of enzyme-dissociated pig stomach showed that single smooth muscle cells containing 95% of the myosin with insert shortened nearly three times faster than cells containing 38% of this myosin type (Eddinger and Meer, 2001). Nevertheless, this range of performance is insufficient to account for the velocities measured in tissues, indicating that myosin tailpiece variation or other factors in the cell impact upon performance. Our study confirms previous work (Kelley et al., 1992) showing that monomeric SM1 and SM2 myosins move actin filaments with the same velocity in vitro, refuting the notion that the tailpieces might directly affect mechanical interaction with actin. However, because they affect thick filament stability and geometry, the tailpieces could influence cellular mechanics by an indirect mechanism. Because this has not previously been addressed, we expressed homogeneous populations of recombinant molecules and assessed their performance using sensitive assays specific for filament assembly, allowing us to uncover subtle but significant functional differences between the carboxyl-terminal isoforms.

Molecular packing in paracrystals

The most convincing demonstration that the tailpiece isoforms affect the packing of molecules in the filament came from the distinct paracrystalline arrays formed from the expressed rod fragments containing either the SM1 or SM2 tailpiece. By interpreting the negative staining pattern in terms of stain accumulation (representing gaps between molecules) and stain exclusion (due to molecular overlaps), distinct models for the molecular packing of the two species can be proposed (Fig. 3). To account for the 64.5-nm period observed for SM1, adjacent molecules are axially staggered by 64.5 nm, consisting of a 43-nm overlap and a 21.5-nm gap (Fig. 3 A, bottom). In this type of model, the length of the molecule is an integral multiple of the period plus the overlap distance (Kendrick-Jones et al., 1969), thus the SM1 rods are proposed to be $(2 \times 64.5) + 43 = 172$ nm in length. Both of our constructs have 1,083 amino acid residues in the coiled-coil region preceding the tailpiece, not including the HIS tag, so at 1.48-Å axial rise per residue in the α-helical myosin coiled coil, they should be at least 161 nm long. The similarity of this value to the length predicted above argues for the applicability of the model.

The packing for SM2 is quite different (Fig. 3 B). Here the rods are staggered by a single 43-nm antiparallel overlap,

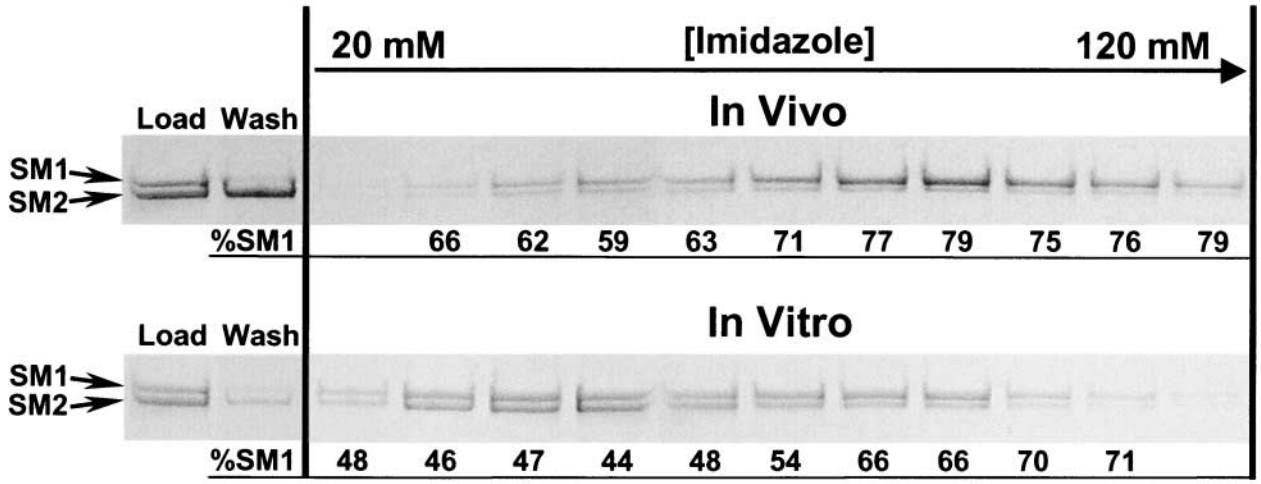

Figure 8. **Comparison of SM1/SM2 rod heterodimer formation in vivo versus in vitro.** Separation of SM1 and SM2 rod heavy chains in homo- and heterodimers eluted from IMAC columns on 3–8% acrylamide gradient SDS gels. (Top) Load, 10 mM imidazole wash, and 11 fractions eluted by an imidazole gradient from a column loaded with partially purified native rods from cells coinfected with tagged rod SM1 and untagged SM2. (Bottom) Equivalent experiment for same starting material after it was denatured in Gu-HCl, then renatured by dialysis. SM1/SM2 heterodimers elute earlier in the imidazole gradient than SM1 homodimers. Comparable elution patterns were obtained in two other experiments. Numbers below gel lanes refer to the percentage of SM1 in each fraction.

with only small (<1 nm) gaps between molecules. In a single segment, this arrangement leads to a structure with a central light-staining 43-nm band flanked by two wider regions of ~114 nm, at the ends of which are two ragged 43-nm "carpet fringes" caused by the axial stagger of the ends of the two sets of rod molecules (Fig. 3 B, bottom). The longer structure we observed with repetitive, alternating 43- and 110-nm period lengths could be produced by end-to-end annealing of these single units to produce a compound segment (Fig. 3 B, bottom, vertical arrow). These structures are identical to those reported for single and compound paracrystalline segments of proteolytically derived rod from chicken gizzard myosin (Kendrick-Jones et al., 1971). Because the carboxyl-terminal tail of smooth myosin can be easily removed during the proteolytic cleavage to form LMM or rod (Ikebe et al., 1991; unpublished data), it is not surprising that paracrystals formed by our expressed tailless constructs, or SM2 rods, with their very short tailpiece, pack similarly to the tissue-derived molecules. The paracrystal data suggest that the different tailpieces of SM1 and SM2 influence the packing of myosin molecules in the smooth muscle thick filament.

Validity of rod as a model system

Even though the rod constructs provided valuable information on the molecular packing of the SM1 and SM2 isoforms, it was important to establish that their assembly properties accurately reflect the properties of their cognate whole myosin molecules. Although low yields precluded a complete analysis, we were able to prepare enough of the myosin isoforms to demonstrate convincingly that their relative behaviors were the same as those of the rod fragments. Most importantly, the several-fold lower critical concentration of SM1 myosin confirmed that it forms more stable filaments than SM2 under reasonably physiological conditions, as was the case for rod SM1 and SM2. The recombinant myosins, when applied to the flow cell in monomeric form, moved actin in the motility assay at rates comparable to those obtained from tissue-purified myosin, or expressed HMM constructs (Fig. 7). This is the first time a full-length vertebrate myosin with uncompromised function has been successfully expressed. Our finding that the velocities supported by SM1 and SM2 myosins were not different argues that the tailpieces do not exert a direct, intramolecular effect on the inherent kinetics of the molecule, reproducing earlier results (Kelley et al., 1992).

Preference for homodimers

The potential impact of the two tailpieces on smooth muscle function would be less if significant quantities of the SM1/SM2 heterodimer exist in cells, because this would decrease the potential number of filaments containing predominantly either SM1 or SM2 myosin. This situation is possible, as the mRNA for the two isoforms is coexpressed in single cells (Eddinger and Meer, 2001). When the amount of heterodimer formed by coassembly within Sf 9 cells was compared with that obtained from denaturation and renaturation of the same starting material, we observed a distinct preference for the formation of homodimers in vivo. The amount of rod heterodimer formed after renaturation in vitro was consistent with random association of the SM1 and SM2 heavy chains, indicating that a coiled-coil species with heterologous tailpieces is as stable as one where the tailpieces are the same.

Our observation of preferential homodimer formation in vivo is consistent with previous work, where myosin from smooth muscle tissue was fractionated using tailpiece-specific antibodies (Kelley et al., 1992). These investigators saw no evidence for more than trace amounts of SM1/SM2 heterodimers in bovine aorta or chicken gizzard myosin. Such results may initially be surprising, because the entire sequence of the coiled coil up to the tailpiece is identical in

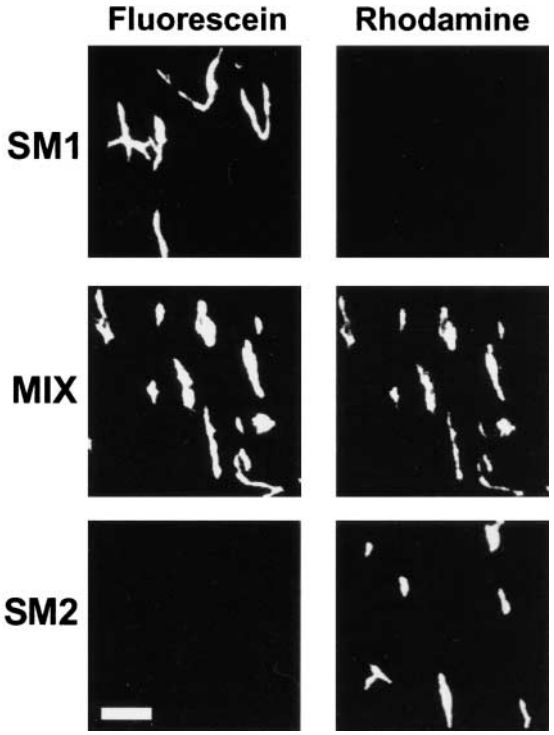

Figure 9. **Formation of heterogeneous thick filaments in vitro by Rod SM1 and SM2.** Fluorescent filaments formed from SM1, SM2, or the mixture of the two were observed with filter sets specific for fluorescein or rhodamine emission, and filament images were captured as described in Materials and methods. Bar, 20 μm.

both isoforms. However, other work using coinfection of multiple viruses in insect cells has shown that it is possible to express reasonable quantities of heterodimeric HMMs which differ in the motor domain, but have identical subfragment 2 regions, where the two heads intertwine (Sweeney et al., 2000; Rovner et al., 2001). This argues against the idea that preferential formation of homodimers in vivo occurs by some sort of spatial separation of mRNAs. A more likely explanation is that the heavy chains immediately associate as they are synthesized on polysomes, and that the stable nature of the full-length coiled-coil rod prevents extensive dissociation and exchange with other myosin isoforms. The shorter HMM molecule, which lacks the stabilizing influence of the extended coiled coil, dissociates to a monomeric subfragment 1–like molecule to a significant extent in benign solvents (Trybus, 1994). Therefore, HMM might be expected to undergo extensive subunit exchange after synthesis, generating a random population of homodimers and heterodimers.

Homodimeric myosins are also preferentially formed in invertebrates such as *Caenorhabditis elegans* (Miller et al., 1983) and in vertebrate skeletal muscles, where different developmental heavy chain isoforms are the products of separate genes in the multinucleated cells (Lowey et al., 1991). When bacterially expressed LMM fragments of the adult and neonatal isoforms were denatured and renatured in vitro, they preferentially formed homodimers, indicating that the information for skeletal myosin formation probably is inherent in the amino acid sequence (Arrizubieta and Bandman, 1999). In contrast, mammalian cardiac muscle contains amounts of heterodimeric V2 myosin comparable to those of the homodimeric V1 and V3 forms during certain stages of development (Hoh et al., 1978; Lompre et al., 1979). This suggests that any V2 formed by limited subunit exchange between the homodimers is extremely stable and will not subsequently reexchange. A striking example of this type of heterodimer stability occurs in tropomyosin, where the more stable αβ molecule was formed at elevated temperatures from the αα and ββ molecules by subunit exchange (Lehrer et al., 1989).

Our analysis of the filaments formed by mixtures of the two labeled rods clearly showed they can copolymerize into heterogeneous thick filaments in vitro (Fig. 9). Therefore, the preferential formation of homodimers of myosin molecules in vivo does not ensure that thick filaments containing predominantly one isoform or the other will be formed. There is currently no evidence for homogeneous thick filaments in smooth muscle tissues which express both isoforms.

Filament assembly

The unique paracrystalline packing and decreased critical concentration of SM1 rod indicates that the longer tailpiece confers greater stability on filaments than the shorter SM2 structure. The reason for this may be that the SM2 sequence, with its three consecutive Pro residues (Fig. 1), creates a kinked, rigid structure that presents greater steric interference to adjacent monomers than the longer and potentially more flexible SM1. SM1 usually appears earlier in postnatal development (Mohammad and Sparrow, 1988; Eddinger and Wolf, 1993) and is better maintained in cell culture than SM2 (Rovner et al., 1986a). This preferential expression of the isoform which is more adept at assembly would be quite advantageous to the cell, as it would allow the formation of thick filaments even during those times when minimal total amounts of myosin are available.

A previous study that used bacterial expression of nonmuscle LMM fragments concluded that the nonhelical tailpiece enhances filament formation, as removal of this SM1-like structure greatly increased the critical concentration for assembly. These workers proposed that the tailpiece promotes assembly by forcing an optimal degree of stagger between adjacent molecules and sterically blocking unproductive molecular interactions in the filament (Hodge et al., 1992). However, our results showed that the tailless mutant assembles as well as or better then the long-tailed SM1 isoform, consistent with the finding that chymotryptic removal of the tailpieces from tissue-purified whole smooth muscle myosin enhanced assembly (Ikebe et al., 1991). Either the smaller LMM fragments give results that differ from whole myosin or rod, and/or scattered differences in sequence between smooth and nonmuscle myosin heavy chains differentially affect the function of similar tailpieces.

It has been proposed that the in vitro assembly of smooth muscle thick filaments occurs via a two-step nucleation/elongation mechanism, where nucleation involves the antiparallel association of two molecules, and elongation occurs by the addition of single monomers to filament ends (Cross et al., 1991). Critical concentration measurements reveal the propensity of molecules to form the initial nucleating spe-

cies, and in our case, indicate that SM1 and TL are more adept at this than SM2. Filament-length assessments suggest that SM1 and SM2 are equally well adapted for addition to preexisting filament ends at pH 7.5 in the presence of Mg^{2+}, whereas SM1 is slightly favored at the more stringent pH 8.0. TL forms longer filaments which are more heterogeneously distributed at either pH. These observations suggest that the tailpieces inhibit elongation to some extent, and help to ensure that filaments polymerize with a narrow distribution of lengths.

Differences in the lengths of thick filaments formed by different myosin isoforms could ultimately lead to changes in the velocity of cell shortening by causing alterations in the dimensions of the basic contractile unit, the sarcomere. For instance, in a contractile structure of set length within the cell (ie., a myofibril), shorter sarcomeres would allow more of these contractile units with finite velocities of shortening to be linked in series, allowing faster cell shortening by the summation of the individual shortening velocities of each sarcomere. However, in our analysis, the lengths of the filaments formed by the SM1 and SM2 isoforms differed very little, and certainly could not account for the range of tissue shortening velocities for different smooth muscle tissues, even when the twofold effect of the ATP-binding pocket insert is considered.

What may be more important are the intermolecular effects that the tailpiece isoforms have on the kinetics or regulation of neighboring molecules within the thick filament. This paradigm is prevalent in the nonmuscle myosin II isoforms such as *Acanthamoeba*, where phosphorylation of three serine residues in the nonhelical tailpiece at the carboxyl terminus of the molecule inhibits the actin-activated ATPase activity of thick filaments (Collins et al., 1982). Presumably, this occurs by an increase in the flexibility of a specific hinge site in the tail and interaction with neighboring molecules (Rau et al., 1993). In smooth muscle, one report suggested that the extended tailpiece of SM1 binds to the subfragment-2/LMM hinge region of an adjacent molecule in the thick filament, slowing contraction velocity (Cai et al., 1995). Although the chicken gizzard SM1 used in this study lacks the casein kinase II consensus site, it is possible that phosphorylation of this site in mammalian myosins could modulate the putative intermolecular interaction described above. In this light, it seems reasonable to suppose that the differences in thick filament packing caused by the SM1 and SM2 tailpieces could influence the potential interactions between molecules within the filament that might alter their enzymatic and motile activities, irrespective of length or thickness of the whole filament. Further work that focuses on these intermolecular effects and their regulation will allow us to better understand whether the properties of smooth muscle isoforms can be primarily responsible for the tremendous range of smooth muscle contractile performance.

Materials and methods

DNA construction and production of recombinant baculoviruses

A full-length chicken gizzard myosin heavy chain cDNA (Yanagisawa et al., 1987) ending with SM1 tailpiece sequence containing 44 rather than the 43 amino acids found in rat and rabbit was used in this study (Fig. 1). The SM2 heavy chain was created by replacing the tailpiece sequence with that of the rabbit SM2 isoform, whereas a truncated tailless mutant was constructed by placing a stop codon after Arginine 1,935, the last residue before the alternative splice site (Fig. 1).

The baculoviral transfer plasmid pAcSG2 (PharMingen) was modified in the multiple cloning region to include sequence for an amino-terminal FLAG epitope tag (DYKDDDDK) followed by an NcoI site. An NcoI site was added within the initial ATG codon of myosin heavy chain cDNAs, allowing ligation into the modified plasmid to yield amino-terminal sequence of MDYKDDDDKA-MAQK... versus the wild-type myosin initial sequence of MSQK... For rod fragments, pAcSG2 was engineered to include initiating sequence encoding an HIS tag followed immediately by a BstEII restriction site. Heavy chain cDNAs were restricted at a naturally occurring BstEII site in the codon for Val853 and ligated into the plasmid, yielding molecules with initial sequence of MHHHHHHAM-V, followed by 1,082 residues of α-helical sequence. Each construct in pAcSG2 was transfected and amplified in Sf 9 cells by established methods (O'Reilly et al., 1992). To produce protein, myosin heavy chain viruses were coinfected along with a recombinant virus encoding both the smooth muscle myosin essential and regulatory light chains (Rovner et al., 1997), whereas rod viruses were used alone.

Protein preparation

After 3 d of infection, Sf 9 cells were lysed, and their contents were fractionated by successive ammonium sulfate precipitations (Trybus, 1994). Different protocols were used from this point to purify myosin versus rod constructs. For the former, the pellet from the 40–70% ammonium sulfate fraction was dialyzed overnight against a buffer containing 90 mM NaCl, 10 mM Na-PO_4, pH 7.4 at 4°C, 1 mM DTT, and 0.1 mM MgATP. Additional ATP was then added to 2 mM, and the material was clarified and applied to a small anti-FLAG affinity column (Sepharose-linked anti-FLAG M2 antibody; Sigma-Aldrich). After washing, elution was carried out with a high-salt buffer (0.5 M NaCl, 20 mM Na-PO_4, pH 7.4 at 4°C) containing FLAG peptide at a concentration of 0.1 mg/ml. Peak fractions were pooled, DTT was added to 1 mM, and the protein was concentrated in one of two ways. In some cases, glucose (10 mM) and hexokinase (20 U/ml; Sigma-Aldrich) were added to remove ATP, the myosin was pelleted with F-actin (0.1 mg/ml), washed, and then released by the addition of 0.5 mM MgATP. In other experiments, FLAG column elution pools were concentrated by ultrafiltration (Centricon-30; Amicon). These preparations typically yielded ~100–200 μg of purified full-length myosin per 10^9 infected cells.

For rod constructs, the 40–70% ammonium sulfate pellets were dialyzed sequentially versus buffers containing (a) 0.5 M NaCl, 20 mM Na-PO_4, pH 8.0 at 4°C, 1 mM DTT, and 1 μg/ml leupeptin; and (b) 0.5 M NaCl, 10 mM MOPS, pH 8.0 at 4°C, 50 mM imidazole, and leupeptin. This material was clarified, loaded onto an immobilized metal-chelate affinity column (IMAC) (Probond; Invitrogen), washed with loading buffer, and then eluted with 25 volumes of a linear imidazole gradient from 50–300 mM in 0.5 M NaCl, 10 mM MOPS. Peak fractions were pooled, DTT was added to 1 mM, and expressed rod was precipitated by overnight dialysis versus 15 mM NaCl, 20 mM MES, pH 6.6 at 4°C, 1 mM EGTA, 20 mM $MgCl_2$, and 1 mM DTT. After collection by centrifugation, the rod pellet was resuspended in storage buffer (0.45 M NaCl, 10 mM imidazole-HCl, pH 8.0 at 4°C, 1 mM EGTA, 1.5 mM NaN_3, and 1 mM DTT), and then dialyzed against the same. After clarification (18 min at 95,000 rpm) (TLA100.2 rotor; Beckman Coulter), purified rod aliquots were frozen in liquid nitrogen and stored at −80°C. These preparations generally yielded 1.5 mg of protein for 10^9 infected cells.

After column purification, the TL preparation contained significant quantities of a lower molecular mass peptide. The TL could be selectively precipitated away from this contaminant by dialysis against a buffer containing 125 mM NaCl, 10 mM Imidazole-HCl, pH 8.0 at 4°C, 1 mM EGTA, and 1 mM DTT. The precipitated material was resuspended in storage buffer, dialyzed, clarified, and stored as above.

Electron microscopy of rod paracrystals and thick filaments

Paracrystalline rod segments were prepared as previously described (Kendrick-Jones et al., 1971), by prolonged dialysis versus a buffer containing 100 mM KSCN, 50 mM Tris-HCl, pH 8.2 at 4°C, 50 mM $CaCl_2$, and 1 mM DTT to induce crystallization. The precipitated material was placed on Formvar-coated, carbon-stabilized copper grids, stained with 1% aqueous uranyl acetate, and viewed with a JEOL 1210 transmission electron microscope at magnifications from 15,000 to 80,00× at a voltage of 60 KV. The lengths of light and dark-staining bands were measured using Scion image software (Scion, Inc.) on digital files created from flatbed scans of EM negatives. The accuracy of these lengths was verified by comparison with tropomyosin paracrystals, which have a repeat distance of 395 Å.

Thick filaments of SM1 and SM2 myosin or the three different rod fragments were prepared by rapid threefold dilution of monomeric protein in storage buffer (see next section). The structures were stained and viewed in the electron microscope, and length measurements were obtained as above. Length–frequency histograms were constructed on a minimum of 315 filaments for each species, using bin sizes of 50 nm. The average length and standard deviation of the filament populations were calculated, and they were then compared against each other by an unpaired, two-tailed *t* test. *P* values <0.05 were deemed significant.

Salt curve analyses

Salt-dependent solubility was assessed with a buffer containing various concentrations of NaCl, 10 mM Imidazole-HCl, 1 mM EGTA, 1.5 mM NaN_3, and 1 mM DTT. We used a pH of 7.5 and added 4 mM $MgCl_2$ to enhance filament assembly in some assays, or a pH of 8.0 without added $MgCl_2$ to discourage it in other assays.

Polymerization was induced by rapid dilution or dialysis. For the former, proteins in storage buffer were diluted threefold with buffers containing decreasing concentrations of NaCl to yield samples with the same final protein concentrations, at final NaCl concentrations from 100–450 mM. The concentrations of diluted proteins were ~125 μg/ml for myosin and ~200 μg/ml for rod preparations. In dialysis experiments, multiple aliquots of protein (60–100 μl) in storage buffer were dialyzed for ≥6 h in separate small units (dispo-Biodialyzers; Nest group) against different buffers containing the desired final NaCl concentrations. After dilution or dialysis, each sample was centrifuged 18 min at 95,000 rpm in a Beckman TL-100 ultracentrifuge, the supernatant was withdrawn, and prepared for SDS gel electrophoresis. In some cases, BSA was also included at 0.5 mg/ml in dilution and dialysis buffers to limit non-specific binding to centrifuge tubes. The values of relative solubility for unknowns were calculated by comparison of their gel staining intensity (see "Gel electrophoresis" below) with a control sample of equal concentration which was diluted with (or dialyzed against) storage buffer and then treated identically. Generally, the amount of protein recovered in the supernatant of this control was 80–90% of the total amount of protein in the tube before centrifugation. These solubilities were plotted as a function of NaCl concentration, and the data was fit using a sigmoidal equation (Slidewrite). Results obtained by dilution or dialysis were similar, allowing pooling of data obtained by both methods.

Critical concentration measurements

For the determination of the critical concentration for filament assembly, rod proteins were adjusted to different starting concentrations using storage buffer to maintain their monomeric state. They were then quickly diluted threefold using a buffer containing 10 mM Imidazole-HCl, pH 8.0, 1 mM EGTA, and 1 mM DTT (dilution buffer). Samples were centrifuged using the parameters described above for salt curve analysis. Aliquots were taken from the total sample before and the supernatant after centrifugation for quantification by gel electrophoresis (see next section). The amount of monomeric rod in each supernatant was plotted as a function of the total amount of rod in each sample before centrifugation. Data for each construct was fitted with the linear equation $y = mx + b$ for the plateau values of x, where the intercept of the latter equation described the value of critical concentration. Alternatively, monomeric samples were dialyzed against dilution buffer containing 150 mM NaCl, then treated as just described. This method gave comparable results to dilution, hence, data obtained from experiments using either method were pooled. For quantification of full-length myosin samples, an ammonium ATPase assay (Rovner et al., 1997) was used.

Gel electrophoresis and quantification of solubility

All gel electrophoresis was by the method of Laemmli (Laemmli, 1970). For separation of expressed isoforms of the full-length myosin heavy chain, 3.5% acrylamide SDS gels were used (Rovner et al., 1986b), whereas 5% gels were used to examine homodimeric rod preparations. Western blotting on 5% acrylamide gels used a monoclonal antibody against rabbit SM2, provided by Dr. Ryozo Nagai (Tokyo University, Tokyo, Japan). To separate the heavy chains of homo- and heterodimer rod mixtures, 3–8% gradient NuPage precast gels were used (Invitrogen).

For the quantitative analysis of samples from rod salt curves and critical concentration experiments, the staining intensity of unknown samples run on 9 or 10% acrylamide gels was compared with a standard curve of smooth muscle myosin purified from turkey gizzard run on the same gel. The KODAK EDAS 120 system, consisting of a digital camera and proprietary software, was used for this purpose.

Actin filament motility

Purified myosins were first phosphorylated by the addition of MgATP, Ca^{2+}, calmodulin, and myosin light chain kinase at concentrations of 1.0 mM, 1.5 mM, 7.5 μg/ml, and 10 μg/ml respectively, followed by incubation for >1 h on ice. In vitro measurements of the velocity of unloaded actin filament movement by monomeric myosin was as described by Rovner et al. (1997).

Assessment of rod heterodimer formation

Experiments investigating the formation of the SM1/SM2 heterodimer used an untagged rod SM2 construct whose initial sequence M-VTR... faithfully reproduced the myosin rod sequence beginning with Valine 853. Sf9 cells were coinfected with viruses for HIS-tagged rod SM1 and this untagged rod SM2 in ratios predetermined to give nearly equal expression of the two heavy chain fragments. The total rod population was partially purified from these cells by ammonium sulfate fractionation, resuspension in a high-salt buffer, and precipitation by dialysis against the low-salt MES buffer previously described. In three separate experiments, ratios from 38% SM1:62% SM2 to 49% SM1:51% SM2 were obtained upon densitometric scanning of gels run on these total rod preparations. The precipitate (>90% rod protein by gel electrophoresis) was collected by centrifugation, and then resuspended in a buffer containing 0.5 M NaCl, 10 mM MOPS, pH 8.0 at 4°C, 1 mM EGTA, and 1 mM DTT. 5 mg of this native rod preparation was loaded on a 5-ml ProBond column, and washed with loading buffer. An additional wash with the same buffer containing 10 mM imidazole was then used to remove nonspecifically bound SM2 rod homodimer. Finally, the column was eluted with a 125-ml gradient from 10 to 300 mM imidazole in loading buffer. Wash and elution fractions were then analyzed by SDS-PAGE.

To determine whether coiled-coil formation would be random in vitro, an aliquot of the native rod preparation from above was denatured by the addition of solid Gu-HCl to a final concentration of 8 M, and DTT was added to 5 mM. The dissociated rod heavy chains were then exhaustively dialyzed against the 0.5 M NaCl HIS column loading buffer with 1 mM DTT to allow reformation of coiled coils. 5 mg of the denatured–renatured material was loaded onto a fresh 5-ml IMAC column, which was washed and eluted identically to the native material.

Formation of heterogeneous thick filaments by labeled, expressed rods

Purified rod SM1 and SM2 were labeled with iodoacetamidofluorescein and tetramethyl-rhodamine-5-iodoacetamide, respectively, by established protocols (Molecular Probes). Homogeneous preparations of monomeric, labeled SM1 and SM2, as well as an equal mixture of the two isoforms, were dialyzed at a concentration of 0.175 mg/ml against a buffer formulated to produce very long filaments which could be visualized by light microscopy containing 100 mM NaCl, 10 mM MES, pH 6.5 at 4°C, 5 mM $MgCl_2$, and 1 mM DTT. These preparations were observed on a Zeiss Axiovert 10 epiflourescence microscope with a 40× objective, using fluorescein and rhodamine filters. Images were obtained from an intensified CCD camera and stored on videotape. Still fields were then obtained as JPEG files by frame grabbing using a WINTV-GO model 190 video card (Hauppaugge, Inc.).

The authors wish to thank Dr. Ryozo Nagai for the generous gift of monoclonal antibody versus the SM2 tailpiece, and Steve Work of the Department of Physiology for help with frame grabbing.

This work was supported in its early stages by a grant-in-aid to A. Romer from the American Heart Association, and by the National Institutes of Health (grants HL38113 and HL54568 to K. Trybus, and AR17350 to S. Lowey).

Submitted: 30 July 2001
Revised: 28 November 2001
Accepted: 28 November 2001

References

Arrizubieta, M.J., and E. Bandman. 1999. Regulation of alpha-helical coiled-coil dimerization in chicken skeletal muscle light meromyosin. *J. Biol. Chem.* 274:13847–13853.

Atkinson, M.A.L., and E.D. Korn. 1987. A model for the polymerization of *Acanthamoeba* myosin II and the regulation of its actin-activated Mg^{2+}-ATPase activity. *J. Biol. Chem.* 262:15809–15811.

Babij, P., and M. Periasamy. 1989. Myosin heavy chain isoform diversity in smooth muscle is produced by differential RNA processing. *J. Mol. Biol.* 210:673–679.

Barany, M. 1967. ATPase activity of myosin correlated with speed of muscle shortening. *J. Gen. Physiol.* 50:197–216.

Cai, S., D.G. Ferguson, A.F. Martin, and R.J. Paul. 1995. Smooth muscle contractility is modulated by myosin tail-S2-LMM hinge region interaction. *Am. J. Physiol.* 269:C1126–C1132.

Collins, J.H., G.P. Cote, and E.D. Korn. 1982. Localization of the three phosphorylation sites on each heavy chain of *Acanthamoeba* myosin II to a segment at the end of the tail. *J. Biol. Chem.* 257:4529–4534.

Cross, R.A., M.A. Geeves, and J. Kendrick-Jones. 1991. A nucleation-elongation mechanism for the self-assembly of side polar sheets of smooth muscle myosin. *EMBO J.* 10:747–756.

Eddinger, T.J., and J.A. Wolf. 1993. Expression of four myosin heavy chain isoforms with development in mouse uterus. *Cell. Motil. Cytoskel.* 25:358–369.

Eddinger, T.J., and D.P. Meer. 2001. Single rabbit stomach smooth muscle cell myosin heavy chain SMB expression and shortening velocity. *Am. J. Physiol.* 280:C309–C316.

Hodge, T.P., R. Cross, and J. Kendrick-Jones. 1992. Role of the COOH-terminal nonhelical tailpiece in the assembly of a vertebrate nonmuscle myosin rod. *J. Cell Biol.* 118:1085–1095.

Hoh, J.F., P.A. McGrath, and P.T. Hale. 1978. Electrophoretic analysis of multiple forms of rat cardiac myosin: effects of hypophysectomy and thyroxine replacement. *J. Mol. Cell Cardiol.* 10:1053–1076.

Ikebe, M., T.E. Hewett, A.F. Martin, M. Chen, and D.J. Hartshorne. 1991. Cleavage of a smooth muscle Myosin heavy chain near its COOH terminus by α-chymotrypsin. Effect on the properties of myosin. *J. Biol. Chem.* 266: 7030–7036.

Kawamoto, S., and R.S. Adelstein. 1988. The heavy chain of smooth muscle myosin is phosphorylated in aorta cells. *J. Biol. Chem.* 263:1099–1102.

Kelley, C.A., J.R. Sellers, P.K. Goldsmith, and R.S. Adelstein. 1992. Smooth muscle myosin is composed of homodimeric heavy chains. *J. Biol. Chem.* 267: 2127–2130.

Kelley, C.A., M. Takahashi, J.H. Yu, and R.S. Adelstein. 1993. An insert of seven amino acids confers functional differences between smooth muscle myosins from the intestines and vasculature. *J. Biol. Chem.* 268:12848–12854.

Kendrick-Jones, J., C. Cohen, A.G. Szent-Gyorgyi, and W. Longley. 1969. Paramyosin: molecular length and assembly. *Science.* 163:1196–1198.

Kendrick-Jones, J., A.G. Szent-Gyorgyi, and C. Cohen. 1971. Segments from vertebrate smooth muscle myosin rods. *J. Mol. Biol.* 59:527–529.

Laemmli, U.K. 1970. Cleavage of structural proteins during the assembly of the head of bacteriophage T4. *Nature.* 227:680–685.

Lehrer, S.S., Y. Qian, and S. Hvidt. 1989. Assembly of the native heterodimer of *Rana esculenta* tropomyosin by chain exchange. *Science.* 246:926–928.

Lompre, A.-M., K. Schwartz, A. d'Albis, G. Lacombe, N. Van Thiem, and B. Swynghedauw. 1979. Myosin isoenzyme redistribution in chronic heart overload. *Nature.* 282:105–107.

Lowey, S., G.S. Waller, and E. Bandman. 1991. Neonatal and adult myosin heavy chains form homodimers during avian skeletal muscle development. *J. Cell Biol.* 113:303–310.

Malmqvist, U., and A. Arner. 1991. Correlation between isoform composition of the 17 kDa myosin light chain and maximal shortening velocity in smooth muscle. *Pflugers Arch.* 418:523–530.

Miller, D.M., III, I. Ortiz, G.C. Berliner, and H.F. Epstein. 1983. Differential localization of two myosins within nematode thick filaments. *Cell.* 34:477–490.

Mohammad, M.A., and M.P. Sparrow. 1988. Changes in myosin heavy chain stoichiometry in pig tracheal smooth muscle during development. *FEBS Lett.* 228:109–112.

Murakami, N., V.P. Chauhan, and M. Elzinga. 1998. Two nonmuscle myosin II heavy chain isoforms expressed in rabbit brains: filament forming properties, the effects of phosphorylation by protein kinase C and casein kinase II, and location of the phosphorylation sites. *Biochemistry.* 37:1989–2003.

Murphy, R.A., J.S. Walker, and J.D. Strauss. 1997. Myosin isoforms and functional diversity in vertebrate smooth muscle. *Comp. Biochem. Physiol. B. Biochem. Mol. Biol.* 117:51–60.

Nagai, R., M. Kuro-o, P. Babij, and M. Periasamy. 1989. Identification of two types of smooth muscle myosin heavy chain isoforms by cDNA cloning and immunoblot analysis. *J. Biol. Chem.* 264: 9734–9737.

O'Halloran, T.J., S. Ravid, and J.A. Spudich. 1990. Expression of *Dictyostelium* myosin tail segments in *Escherichia coli*: domains required for assembly and phosphorylation. *J. Cell Biol.* 110:63–70.

O'Reilly, D.R., L.K. Miller, and V.A. Luckow. 1992. Baculovirus expression vectors. A laboratory manual. W.H. Freeman and Co., New York. 347 pp.

Rau, D.C., C. Ganguly, and E.D. Korn. 1993. A structural difference between filaments of phosphorylated and dephosphorylated *Acanthamoeba* myosin II revealed by electric birefringence. *J. Biol. Chem.* 268:4612–4624.

Rovner, A.S., R.A. Murphy, and G.K. Owens. 1986a. Expression of smooth muscle and non-muscle myosin heavy chains in cultured vascular smooth muscle cells. *J. Biol. Chem.* 261:14740–14745.

Rovner, A.S., M.M. Thompson, and R.A. Murphy. 1986b. Two different heavy chains are found in smooth muscle myosin. *Am. J. Physiol.* 25:C861–C870.

Rovner, A.S., Y. Freyzon, and K.M. Trybus. 1997. An insert in the motor domain determines the functional properties of expressed smooth muscle myosin isoforms. *J. Muscle Res. Cell Motil.* 18:103–110.

Rovner, A.S., M. Fagnant, and K.M. Trybus. 2001. Biophysical Society Meeting. 2606 (Abstr.).

Sathyamoorthy, V., M.A.L. Atkinson, B. Bowers, and E.D. Korn. 1990. Functional consequences of the proteolytic removal of regulatory serines from the non-helical tailpiece of *Acanthamoeba* myosin II. *Biochemistry.* 29:3792–3797.

Sweeney, H.L., L.Q. Chen, and K.M. Trybus. 2000. Regulation of asymmetric smooth muscle myosin II molecules. *J. Biol. Chem.* 275:41273–41277.

Trybus, K.M. 1994. Regulation of expressed truncated smooth muscle myosins. Role of the essential light chain and tail length. *J. Biol. Chem.* 269:20819–20822.

Tsao, A.E., and T.J. Eddinger. 1993. Smooth muscle myosin heavy chains combine to form three native myosin isoforms. *Am. J. Physiol.* 264:H1653–H1662.

Yanagisawa, M., Y. Hamada, Y. Katsuragawa, M. Imamura, T. Mikawa, and T. Masaki. 1987. Complete primary structure of vertebrate smooth muscle myosin heavy chain deduced from its complementary DNA sequence. Implications on topography and function of myosin. *J. Mol. Biol.* 198: 143–157.